Observation of an Energy-Dependent Difference in Elliptic Flow between Particles and Antiparticles in Relativistic Heavy Ion Collisions

(STAR Collaboration) Adamczyk, L.; ...; Planinić, Mirko; ...; Poljak, Nikola; ...; Zyzak, M.

Journal article, Published version
Rad u časopisu, Objavljena verzija rada (izdavačev PDF)

Permanent link / Trajna poveznica: https://urn.nsk.hr/urn:nbn:hr:217:072996

Download date / Datum preuzimanja: **2024-04-27**

Repository / Repozitorij:

Repository of the Faculty of Science - University of Zagreb

Observation of an Energy-Dependent Difference in Elliptic Flow between Particles and Antiparticles in Relativistic Heavy Ion Collisions

L. Adamczyk,[1] J. K. Adkins,[23] G. Agakishiev,[21] M. M. Aggarwal,[34] Z. Ahammed,[53] I. Alekseev,[19]
J. Alford,[22] C. D. Anson,[31] A. Aparin,[21] D. Arkhipkin,[4] E. Aschenauer,[4] G. S. Averichev,[21] J. Balewski,[26]
A. Banerjee,[53] Z. Barnovska,[14] D. R. Beavis,[4] R. Bellwied,[49] M. J. Betancourt,[26] R. R. Betts,[10] A. Bhasin,[20]
A. K. Bhati,[34] P. Bhattarai,[48] H. Bichsel,[55] J. Bielcik,[13] J. Bielcikova,[14] L. C. Bland,[4] I. G. Bordyuzhin,[19]
W. Borowski,[45] J. Bouchet,[22] A. V. Brandin,[29] S. G. Brovko,[6] E. Bruna,[57] S. Bültmann,[32] I. Bunzarov,[21]
T. P. Burton,[4] J. Butterworth,[40] X. Z. Cai,[44] H. Caines,[57] M. Calderón de la Barca Sánchez,[6] D. Cebra,[6]
R. Cendejas,[35] M. C. Cervantes,[47] P. Chaloupka,[13] Z. Chang,[47] S. Chattopadhyay,[53] H. F. Chen,[42] J. H. Chen,[44]
J. Y. Chen,[9] L. Chen,[9] J. Cheng,[50] M. Cherney,[12] A. Chikanian,[57] W. Christie,[4] P. Chung,[14] J. Chwastowski,[11]
M. J. M. Codrington,[48] R. Corliss,[26] J. G. Cramer,[55] H. J. Crawford,[5] X. Cui,[42] S. Das,[16] A. Davila Leyva,[48]
L. C. De Silva,[49] R. R. Debbe,[4] T. G. Dedovich,[21] J. Deng,[43] R. Derradi de Souza,[8] S. Dhamija,[18] B. di Ruzza,[4]
L. Didenko,[4] F. Ding,[6] A. Dion,[4] P. Djawotho,[47] X. Dong,[25] J. L. Drachenberg,[52] J. E. Draper,[6] C. M. Du,[24]
L. E. Dunkelberger,[7] J. C. Dunlop,[4] L. G. Efimov,[21] M. Elnimr,[56] J. Engelage,[5] G. Eppley,[40] L. Eun,[25]
O. Evdokimov,[10] R. Fatemi,[23] S. Fazio,[4] J. Fedorisin,[21] R. G. Fersch,[23] P. Filip,[21] E. Finch,[57] Y. Fisyak,[4] E. Flores,[6]
C. A. Gagliardi,[47] D. R. Gangadharan,[31] D. Garand,[37] F. Geurts,[40] A. Gibson,[52] S. Gliske,[2] O. G. Grebenyuk,[25]
D. Grosnick,[52] A. Gupta,[20] S. Gupta,[20] W. Guryn,[4] B. Haag,[6] O. Hajkova,[13] A. Hamed,[47] L-X. Han,[44] J. W. Harris,[57]
J. P. Hays-Wehle,[26] S. Heppelmann,[35] A. Hirsch,[37] G. W. Hoffmann,[48] D. J. Hofman,[10] S. Horvat,[57] B. Huang,[4]
H. Z. Huang,[7] P. Huck,[9] T. J. Humanic,[31] G. Igo,[7] W. W. Jacobs,[18] C. Jena,[30] E. G. Judd,[5] S. Kabana,[45]
K. Kang,[50] J. Kapitan,[14] K. Kauder,[10] H. W. Ke,[9] D. Keane,[22] A. Kechechyan,[21] A. Kesich,[6] D. P. Kikola,[37]
J. Kiryluk,[25] I. Kisel,[25] A. Kisiel,[54] S. R. Klein,[25] D. D. Koetke,[52] T. Kollegger,[15] J. Konzer,[37] I. Koralt,[32]
W. Korsch,[23] L. Kotchenda,[29] P. Kravtsov,[29] K. Krueger,[2] I. Kulakov,[25] L. Kumar,[22] M. A. C. Lamont,[4]
J. M. Landgraf,[4] K. D. Landry,[7] S. LaPointe,[56] J. Lauret,[4] A. Lebedev,[4] R. Lednicky,[21] J. H. Lee,[4]
W. Leight,[26] M. J. LeVine,[4] C. Li,[42] W. Li,[44] X. Li,[37] X. Li,[46] Y. Li,[50] Z. M. Li,[9] L. M. Lima,[41] M. A. Lisa,[31]
F. Liu,[9] T. Ljubicic,[4] W. J. Llope,[40] R. S. Longacre,[4] Y. Lu,[42] X. Luo,[9] A. Luszczak,[11] G. L. Ma,[44] Y. G. Ma,[44]
D. M. M. D. Madagodagettige Don,[12] D. P. Mahapatra,[16] R. Majka,[57] S. Margetis,[22] C. Markert,[48] H. Masui,[25]
H. S. Matis,[25] D. McDonald,[40] T. S. McShane,[12] S. Mioduszewski,[47] M. K. Mitrovski,[4] Y. Mohammed,[47]
B. Mohanty,[30] M. M. Mondal,[47] M. G. Munhoz,[41] M. K. Mustafa,[37] M. Naglis,[25] B. K. Nandi,[17] Md. Nasim,[53]
T. K. Nayak,[53] J. M. Nelson,[3] L. V. Nogach,[36] J. Novak,[28] G. Odyniec,[25] A. Ogawa,[4] K. Oh,[38] A. Ohlson,[57]
V. Okorokov,[29] E. W. Oldag,[48] R. A. N. Oliveira,[41] D. Olson,[25] M. Pachr,[13] B. S. Page,[18] S. K. Pal,[53] Y. X. Pan,[7]
Y. Pandit,[10] Y. Panebratsev,[21] T. Pawlak,[54] B. Pawlik,[33] H. Pei,[10] C. Perkins,[5] W. Peryt,[54] P. Pile,[4] M. Planinic,[58]
J. Pluta,[54] N. Poljak,[58] J. Porter,[25] A. M. Poskanzer,[25] C. B. Powell,[25] C. Pruneau,[56] N. K. Pruthi,[34] M. Przybycien,[1]
P. R. Pujahari,[17] J. Putschke,[56] H. Qiu,[25] S. Ramachandran,[23] R. Raniwala,[39] S. Raniwala,[39] R. L. Ray,[48]
C. K. Riley,[57] H. G. Ritter,[25] J. B. Roberts,[40] O. V. Rogachevskiy,[21] J. L. Romero,[6] J. F. Ross,[12] L. Ruan,[4] J. Rusnak,[14]
N. R. Sahoo,[53] P. K. Sahu,[16] I. Sakrejda,[25] S. Salur,[25] A. Sandacz,[54] J. Sandweiss,[57] E. Sangaline,[6] A. Sarkar,[17]
J. Schambach,[48] R. P. Scharenberg,[37] A. M. Schmah,[25] B. Schmidke,[4] N. Schmitz,[27] T. R. Schuster,[15] J. Seger,[12]
P. Seyboth,[27] N. Shah,[7] E. Shahaliev,[21] M. Shao,[42] B. Sharma,[34] M. Sharma,[56] S. S. Shi,[9] Q. Y. Shou,[44]
E. P. Sichtermann,[25] R. N. Singaraju,[53] M. J. Skoby,[18] D. Smirnov,[4] N. Smirnov,[57] D. Solanki,[39] P. Sorensen,[4]
U. G. deSouza,[41] H. M. Spinka,[2] B. Srivastava,[37] T. D. S. Stanislaus,[52] J. R. Stevens,[26] R. Stock,[15] M. Strikhanov,[29]
B. Stringfellow,[37] A. A. P. Suaide,[41] M. C. Suarez,[10] M. Sumbera,[14] X. M. Sun,[25] Y. Sun,[42] Z. Sun,[24] B. Surrow,[46]
D. N. Svirida,[19] T. J. M. Symons,[25] A. Szanto de Toledo,[41] J. Takahashi,[8] A. H. Tang,[4] Z. Tang,[42] L. H. Tarini,[56]
T. Tarnowsky,[28] J. H. Thomas,[25] J. Tian,[44] A. R. Timmins,[49] D. Tlusty,[14] M. Tokarev,[21] S. Trentalange,[7]
R. E. Tribble,[47] P. Tribedy,[53] B. A. Trzeciak,[54] O. D. Tsai,[7] J. Turnau,[33] T. Ullrich,[4] D. G. Underwood,[2]
G. Van Buren,[4] G. van Nieuwenhuizen,[26] J. A. Vanfossen, Jr.,[22] R. Varma,[17] G. M. S. Vasconcelos,[8] F. Videbæk,[4]
Y. P. Viyogi,[53] S. Vokal,[21] S. A. Voloshin,[56] A. Vossen,[18] M. Wada,[48] F. Wang,[37] G. Wang,[7] H. Wang,[4] J. S. Wang,[24]
Q. Wang,[37] X. L. Wang,[42] Y. Wang,[50] G. Webb,[23] J. C. Webb,[4] G. D. Westfall,[28] C. Whitten, Jr.,[7] H. Wieman,[25]
S. W. Wissink,[18] R. Witt,[51] Y. F. Wu,[9] Z. Xiao,[50] W. Xie,[37] K. Xin,[40] H. Xu,[24] N. Xu,[25] Q. H. Xu,[43] W. Xu,[7] Y. Xu,[42]
Z. Xu,[4] L. Xue,[44] Y. Yang,[24] Y. Yang,[9] P. Yepes,[40] L. Yi,[37] K. Yip,[4] I-K. Yoo,[38] M. Zawisza,[54] H. Zbroszczyk,[54]

J. B. Zhang,[9] S. Zhang,[44] X. P. Zhang,[50] Y. Zhang,[42] Z. P. Zhang,[42] F. Zhao,[7] J. Zhao,[44] C. Zhong,[44] X. Zhu,[50]
Y. H. Zhu,[44] Y. Zoulkarneeva,[21] and M. Zyzak[25]

(STAR Collaboration)

[1]*AGH University of Science and Technology, Cracow, Poland*
[2]*Argonne National Laboratory, Argonne, Illinois 60439, USA*
[3]*University of Birmingham, Birmingham, United Kingdom*
[4]*Brookhaven National Laboratory, Upton, New York 11973, USA*
[5]*University of California, Berkeley, California 94720, USA*
[6]*University of California, Davis, California 95616, USA*
[7]*University of California, Los Angeles, California 90095, USA*
[8]*Universidade Estadual de Campinas, Sao Paulo, Brazil*
[9]*Central China Normal University (HZNU), Wuhan 430079, China*
[10]*University of Illinois at Chicago, Chicago, Illinois 60607, USA*
[11]*Cracow University of Technology, Cracow, Poland*
[12]*Creighton University, Omaha, Nebraska 68178, USA*
[13]*Czech Technical University in Prague, FNSPE, Prague, 115 19, Czech Republic*
[14]*Nuclear Physics Institute AS CR, 250 68 Řež/Prague, Czech Republic*
[15]*University of Frankfurt, Frankfurt, Germany*
[16]*Institute of Physics, Bhubaneswar 751005, India*
[17]*Indian Institute of Technology, Mumbai, India*
[18]*Indiana University, Bloomington, Indiana 47408, USA*
[19]*Alikhanov Institute for Theoretical and Experimental Physics, Moscow, Russia*
[20]*University of Jammu, Jammu 180001, India*
[21]*Joint Institute for Nuclear Research, Dubna 141 980, Russia*
[22]*Kent State University, Kent, Ohio 44242, USA*
[23]*University of Kentucky, Lexington, Kentucky 40506-0055, USA*
[24]*Institute of Modern Physics, Lanzhou, China*
[25]*Lawrence Berkeley National Laboratory, Berkeley, California 94720, USA*
[26]*Massachusetts Institute of Technology, Cambridge, Massachusetts 02139-4307, USA*
[27]*Max-Planck-Institut für Physik, Munich, Germany*
[28]*Michigan State University, East Lansing, Michigan 48824, USA*
[29]*Moscow Engineering Physics Institute, Moscow, Russia*
[30]*National Institute of Science Education and Research, Bhubaneswar 751005, India*
[31]*The Ohio State University, Columbus, Ohio 43210, USA*
[32]*Old Dominion University, Norfolk, Virginia 23529, USA*
[33]*Institute of Nuclear Physics PAN, Cracow, Poland*
[34]*Panjab University, Chandigarh 160014, India*
[35]*Pennsylvania State University, University Park, Pennsylvania 16802, USA*
[36]*Institute of High Energy Physics, Protvino, Russia*
[37]*Purdue University, West Lafayette, Indiana 47907, USA*
[38]*Pusan National University, Pusan, Republic of Korea*
[39]*University of Rajasthan, Jaipur 302004, India*
[40]*Rice University, Houston, Texas 77251, USA*
[41]*Universidade de Sao Paulo, Sao Paulo, Brazil*
[42]*University of Science & Technology of China, Hefei 230026, China*
[43]*Shandong University, Jinan, Shandong 250100, China*
[44]*Shanghai Institute of Applied Physics, Shanghai 201800, China*
[45]*SUBATECH, Nantes, France*
[46]*Temple University, Philadelphia, Pennsylvania 19122, USA*
[47]*Texas A&M University, College Station, Texas 77843, USA*
[48]*University of Texas, Austin, Texas 78712, USA*
[49]*University of Houston, Houston, Texas 77204, USA*
[50]*Tsinghua University, Beijing 100084, China*
[51]*United States Naval Academy, Annapolis, Maryland 21402, USA*
[52]*Valparaiso University, Valparaiso, Indiana 46383, USA*
[53]*Variable Energy Cyclotron Centre, Kolkata 700064, India*
[54]*Warsaw University of Technology, Warsaw, Poland*
[55]*University of Washington, Seattle, Washington 98195, USA*

[56]*Wayne State University, Detroit, Michigan 48201, USA*
[57]*Yale University, New Haven, Connecticut 06520, USA*
[58]*University of Zagreb, Zagreb, HR-10002, Croatia*

Elliptic flow (v_2) values for identified particles at midrapidity in Au + Au collisions, measured by the STAR experiment in the beam energy scan at RHIC at $\sqrt{s_{NN}} = 7.7$–62.4 GeV, are presented. A beam-energy-dependent difference of the values of v_2 between particles and corresponding antiparticles was observed. The difference increases with decreasing beam energy and is larger for baryons compared to mesons. This implies that, at lower energies, particles and antiparticles are not consistent with the universal number-of-constituent-quark scaling of v_2 that was observed at $\sqrt{s_{NN}} = 200$ GeV.

Lattice quantum chromodynamics (QCD) predicts that, at sufficiently high temperatures T and/or high baryonic chemical potentials μ_B, normal nuclear matter will undergo a phase transition to a state of matter where quarks and gluons are deconfined, called the quark-gluon plasma (QGP) [1]. This transition is important for understanding the early evolution of the Universe [2]. A beam energy scan (BES) program [3] has been carried out at the Relativistic Heavy Ion Collider (RHIC) facility to study the QCD phase structure over a large range in T and μ_B.

Particle production in heavy ion collisions with respect to the event plane (EP) can be characterized by the following Fourier expansion:

$$\frac{dN}{d(\phi - \Psi)} \propto 1 + 2 \sum_{n \geq 1} v_n^{\text{obs}} \cos[n(\phi - \Psi)], \qquad (1)$$

where ϕ is the azimuthal angle of the particles, n the harmonic number, v_n^{obs} the observed Fourier coefficient that has to be corrected for the EP resolution to get v_n, and Ψ the reconstructed EP azimuthal angle [4,5]. The second harmonic coefficient is denoted as elliptic flow v_2 [4].

Elliptic flow measurements have been used to conclude that strongly interacting partonic matter is produced in Au + Au collisions at $\sqrt{s_{NN}} = 200$ GeV and that v_2 develops in the early, partonic, stage. This conclusion is based in part on the observed scaling of v_2 versus the transverse momentum p_T, with the number of constituent quarks (NCQ) [6–9] for hadrons at intermediate p_T (2 to 5 GeV/c). Deviations from such a scaling for identified hadron $v_2(p_T)$ at lower beam energies is thus an indication for the absence of a deconfined phase [3].

In a hydrodynamic picture, v_2 arises in noncentral heavy ion collisions due to an initial pressure gradient, which is directly connected to the eccentricity. This leads to particle emission predominantly in the direction of the maximum of the pressure gradient. During the expansion of the system the pressure gradient decreases, which means that elliptic flow primarily probes the early stage of a heavy ion collision.

For Au + Au collisions at $\sqrt{s_{NN}} = 200$ GeV, a mass ordering in $v_2(p_T)$ between the different particle species

was observed at low transverse momenta ($p_T < 2$ GeV/c) [6,10,11]. This behavior can be described by nonviscous hydrodynamic calculations [12–17]. The relative mass ordering can be suppressed by using the reduced transverse kinetic energy ($m_T - m_0$) instead of p_T, with $m_T = \sqrt{p_T^2 + m_0^2}$ and m_0 being the mass of the particle. At large ($m_T - m_0$), a splitting in $v_2(m_T - m_0)$ between baryons and mesons was observed that cannot be described by hydrodynamic calculations. This splitting can be explained, in part, by assuming that the particle production occurs via coalescence of constituent quarks [18].

The v_2 values for $\pi^{\pm}$, $K^{\pm}$, K_S^0, p, $\bar{p}$, ϕ, Λ, $\bar{\Lambda}$, Ξ^-, $\bar{\Xi}^+$, Ω^-, $\bar{\Omega}^+$ measured at midrapidity in minimum bias Au + Au collisions will be reported. The data were recorded by STAR, the Solenoidal Tracker at RHIC, for $\sqrt{s_{NN}} = 7.7$, 11.5, 19.6, 27, 39, and 62.4 GeV in the years 2010 and 2011 as part of the BES program [3].

STAR is a multipurpose experiment at RHIC with a complete azimuthal coverage. The main detectors used for the data analysis were the time-projection chamber (TPC) [19] for tracking and particle identification at pseudorapidities $|\eta| < 1.0$, and the time-of-flight (TOF) detector, which was especially important to identify charged particles at intermediate momenta. A minimum bias trigger was defined using a coincidence of hits in the zero degree calorimeters, vertex position detectors, or beam-beam counters [20,21]. To suppress events from collisions with the beam pipe (radius 3.95 cm), an upper limit cut on the radial position of the reconstructed primary vertex of 2 cm was applied. In addition, the z position of the vertices was limited to values less than ± 70 cm. Collisions within a 0%–80% centrality range of the total reaction cross section were selected for the analysis. The centrality definition is based on a comparison between the measured track multiplicity within $|\eta| < 0.5$ and a Glauber Monte Carlo simulation [20].

The particle identification and yield extraction for long-lived charged hadrons (p, $\bar{p}$, $\pi^{\pm}$, $K^{\pm}$) was based on a combination of the ionization energy loss dE/dx in the TPC, the reconstructed momentum (p), and the squared mass m^2 from the TOF detector [21]. Short-lived particles

that decay within the detector acceptance, such as ϕ, Λ, $\bar{\Lambda}$, Ξ^-, $\bar{\Xi}^+$, Ω^-, $\bar{\Omega}^+$, and K_s^0, were identified using the invariant mass technique. The combinatorial background to the weakly decaying particles like Λ and Ξ was reduced by topological reconstruction. The remaining combinatorial background was fit and subtracted with the mixed event technique [21].

The event plane was reconstructed using the procedure described in Ref. [4]. In order to reduce the effects of nonflow contributions arising mainly from Hanbury-Brown Twiss correlations and Coulomb interactions, the event plane angles were estimated for two subevents separated by an additional η gap instead of using the full TPC event plane method [21]. For such an "η-sub-EP" reconstruction, one uses only the particles from the opposite η hemisphere with respect to the particle of interest and outside of an additional η gap of $|\eta| > 0.05$. The nonflow contributions were studied for the six beam energies by comparing different methods of extracting v_2 for inclusive charged hadrons [20]. The four particle cumulant $v_2\{4\}$ strongly suppresses nonflow contributions. It has been shown that the difference between v_2 (η-sub) and $v_2\{4\}$ is 10%–20% for 19.2, 27, and 39 GeV and decreases with decreasing energy. All observed values (v_2^{obs}) were corrected on an event-by-event basis using the EP resolution [22] that was calculated by comparing the two η-sub-EP angles [20].

For each particle species, the cuts used for particle identification and background suppression were varied to estimate the systematic uncertainties. The errors were also estimated by varying the methods used to flatten the EP, to obtain the yields, and to extract the v_2 values. A more detailed description of the detector setup and the analysis can be found in Ref. [21].

In Fig. 1, the p_T dependence of the proton and antiproton v_2 is shown for Au + Au collisions at $\sqrt{s_{NN}} = 7.7$, 11.5, 27, and 39 GeV. At all energies, the v_2 values increase with increasing p_T. At $p_T = 2$ GeV/c, the magnitude of v_2 for protons increases with energy from about 0.10 at 7.7 GeV to 0.15 at 39 GeV. Lower values of $v_2(p_T)$

are observed for antiprotons compared to protons at all energies. The difference in the v_2 values for protons and antiprotons increases with decreasing beam energy. The lower panels of Fig. 1 show the p_T dependence of the difference in v_2 for protons and antiprotons. No significant p_T dependence is observed, as characterized by the horizontal line fits. The negative values of the antiproton v_2 at low p_T at $\sqrt{s_{NN}} = 11.5$ GeV could be influenced by absorption in the medium [23]. Suppressed or negative v_2 values are also observed at $\sqrt{s_{NN}} = 7.7$ GeV for different centralities [21].

The $v_2(p_T)$ behavior for $\Lambda(uds)$, $\bar{\Lambda}(\bar{u}\bar{d}\bar{s})$ and $\Xi^-(dss)$, $\bar{\Xi}^+(\bar{d}\bar{s}\bar{s})$ is similar to that for protons (uud) and antiprotons ($\bar{u}\bar{u}\bar{d}$). In all cases, the baryon antiparticle v_2 is lower than the corresponding particle v_2. The $v_2(p_T)$ difference for Λ and $\bar{\Lambda}$ is in agreement with previous STAR results at $\sqrt{s_{NN}} = 62.4$ GeV [7]. For the mesons $\pi^+(u\bar{d})$, $\pi^-(\bar{u}d)$, and $K^+(u\bar{s})$, $K^-(\bar{u}s)$, the differences are smaller than those for the baryons (the antiparticle convention from Ref. [24] is used for mesons). At $\sqrt{s_{NN}} = 7.7$ GeV, the $v_2(p_T)$ difference between K^+ and K^- is a factor 5–6 smaller as compared to the baryons, with K^+ having a systematically larger $v_2(p_T)$ than K^-. On the other hand, the $v_2(p_T)$ of the π^- is larger than the $v_2(p_T)$ of the π^+. However, the magnitude of the difference for pions as a function of energy is similar to that for the kaons. The details of the p_T dependence of the difference in v_2 between particles and corresponding antiparticles can be found in Ref. [21].

Figure 2 summarizes the variation of the p_T independent difference in v_2 between particles and corresponding antiparticles with $\sqrt{s_{NN}}$. Here, $v_2(X) - v_2(\bar{X})$ denotes the horizontal line fit values of the difference in $v_2(p_T)$ between particles X (p, Λ, Ξ^-, π^+, K^+) and corresponding antiparticles $\bar{X}$ ($\bar{p}$, $\bar{\Lambda}$, $\bar{\Xi}^+$, π^-, K^-). Larger v_2 values are found for particles than for antiparticles, except for pions, for which the opposite ordering is observed. A monotonic increase of the magnitude of $\Delta v_2 = v_2(X) - v_2(\bar{X})$ with decreasing beam energy is observed. The data can be described by a power-law function.
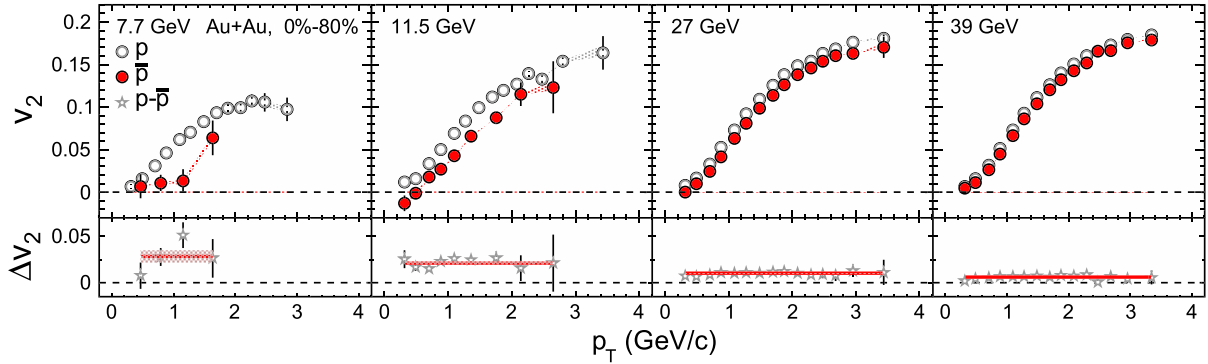

FIG. 1 (color online).   The elliptic flow v_2 of protons and antiprotons as a function of the transverse momentum p_T for 0%–80% central Au + Au collisions. The lower panels show the difference in $v_2(p_T)$ between the particles and antiparticles. The solid curves are fits with a horizontal line. The shaded areas depict the magnitude of the systematic errors.
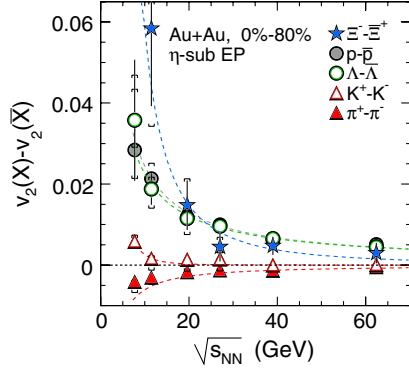
FIG. 2 (color online).   The difference in v_2 between particles (X) and their corresponding antiparticles ($\bar{X}$) (see legend) as a function of $\sqrt{s_{NN}}$ for 0%–80% central Au + Au collisions. The dashed lines in the plot are fits with a power-law function. The error bars depict the combined statistical and systematic errors.

While in Au + Au collisions at $\sqrt{s_{NN}} = 200$ GeV a single NCQ scaling can be observed for particles and antiparticles, the observed difference in v_2 at lower beam energies demonstrates that this common NCQ scaling of particles and antiparticles splits. Such a breaking of the NCQ scaling could indicate increased contributions from hadronic interactions in the system evolution with decreasing beam energy. The energy dependence of $v_2(X) - v_2(\bar{X})$ could also be accounted for by considering an increase in nuclear stopping power with decreasing $\sqrt{s_{NN}}$ if the v_2 of transported quarks (quarks coming from the incident nucleons) is larger than the v_2 of produced quarks [25,26]. Theoretical calculations [27] suggest that the difference between particles and antiparticles could be accounted for by mean field potentials where the K^- and $\bar{p}$ feel an attractive force while the K^+ and p feel a repulsive force.

Most of the published theoretical calculations can reproduce the basic pattern but fail to quantitatively reproduce the measured v_2 difference [25–28]. So far, none of the theory calculations describes the observed ordering of the particles. Therefore, more accurate calculations from theory are needed to distinguish between the different possibilities. Other possible reasons for the observation that the $\pi^- \; v_2(p_T)$ is larger than the $\pi^+ \; v_2(p_T)$ is the Coulomb repulsion of π^+ by the midrapidity net protons (only at low p_T) and the chiral magnetic effect in finite baryon-density matter [29]. Simulations have to be carried out to quantify if those effects can explain our observations.

In Ref. [21], the study of the centrality dependence of Δv_2 for protons and antiprotons is extended to investigate if different production rates for protons and antiprotons as a function of centrality could cause the observed differences. It was observed that the differences, Δv_2, are significant at all centralities.

The $v_2(m_T - m_0)$ and possible NCQ scaling was also investigated for particles and antiparticles separately. Figure 3 shows v_2 as a function of the reduced transverse mass, $(m_T - m_0)$, for various particles and antiparticles at $\sqrt{s_{NN}} = 11.5$ and 62.4 GeV. The baryons and mesons are clearly separated for $\sqrt{s_{NN}} = 62.4$ GeV at $(m_T - m_0) >$ 1 GeV$/c^2$. While the effect is present for particles at $\sqrt{s_{NN}} = 11.5$ GeV, no such separation is observed for the antiparticles at this energy in the measured $(m_t - m_0)$ range up to 2 GeV$/c^2$. The lower panels of Fig. 3 depict the difference of the baryon v_2 relative to a fit to the meson v_2 data with the pions excluded from the fit. The antiparticles at $\sqrt{s_{NN}} = 11.5$ GeV show a smaller difference compared to the particles. At $\sqrt{s_{NN}} = 11.5$ GeV the difference becomes negative for the antiparticles at $(m_T - m_0) < 1$ GeV$/c^2$ but the overall trend is still similar to the one of the particles and to $\sqrt{s_{NN}} = 62.4$ GeV.
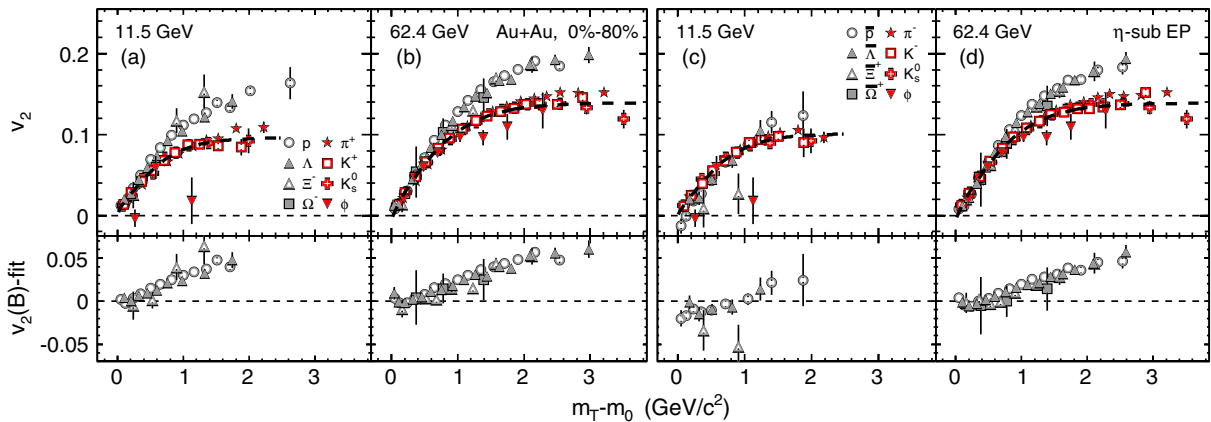

FIG. 3 (color online).   The upper panels depict the elliptic flow v_2 as a function of reduced transverse mass $(m_T - m_0)$ for particles, (a) and (b), and antiparticles, (c) and (d), in 0%–80% central Au + Au collisions at $\sqrt{s_{NN}} = 11.5$ and 62.4 GeV. Simultaneous fits to the mesons except the pions are shown as the dashed lines. The difference of the baryon v_2 and the meson fits are shown in the lower panels.
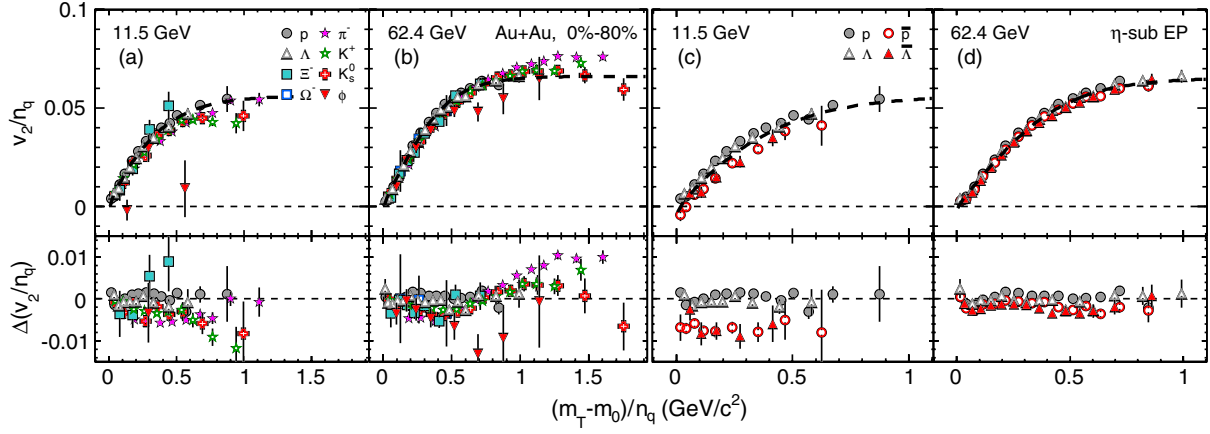
FIG. 4 (color online). The number-of-constituent-quark scaled elliptic flow $(v_2/n_q)((m_T - m_0)/n_q)$ for 0%–80% central Au + Au collisions at $\sqrt{s_{NN}} = 11.5$ and 62.4 GeV for selected particles, (a) and (b), and a direct comparison between selected baryons and antibaryons, (c) and (d). The dashed lines are simultaneous fits [30] to p, $\bar{p}$, Λ, and $\bar{\Lambda}$ at a given energy. The lower panels depict the differences to the fits. Some data points for ϕ are out of the plot range in the lower panels.

In Fig. 4, the $v_2(m_T - m_0)$ values scaled on both axes with the number of constituent quarks are presented for $\sqrt{s_{NN}} = 11.5$ and 62.4 GeV. A simultaneous fit [30] to p, $\bar{p}$, Λ, and $\bar{\Lambda}$ at a given energy is shown as the dashed line. The differences between data and corresponding fits are shown in the lower panels. The general scaling holds, except for the ϕ mesons, for the various particles, as shown in Figs. 4(a) and 4(b) with deviations of $\sim 10\%$ at a $(m_T - m_0)/n_q$ value of 0.7 GeV/c^2. A significant change in the scaling behavior can be observed between baryon and antibaryon v_2 from $\sqrt{s_{NN}} = 62.4$ to 11.5 GeV, as shown in Figs. 4(c) and 4(d). The ϕ mesons are also an exception to the trend of other hadrons. At the highest $(m_T - m_0)/n_q$ values, the ϕ meson data point for $\sqrt{s_{NN}} = 11.5$ GeV ($p_T = 1.9$ GeV/c) is 2.3σ lower than those of the other hadrons. This is comparable to the observed deviation at $\sqrt{s_{NN}} = 7.7$ GeV ($p_T = 1.7$ GeV/c) by 1.8σ [21]. The smaller v_2 values of the $\phi(s\bar{s})$ meson, which has a smaller hadronic interaction cross section [31], may indicate that hadronic interactions become more important than partonic effects for the systems formed at collision energies $\lesssim 11.5$ GeV [32,33].

In summary, the first observation of a beam-energy-dependent difference in $v_2(p_T)$ between particles and corresponding antiparticles for minimum bias $\sqrt{s_{NN}} = 7.7$–62.4 GeV Au + Au collisions at midrapidity is reported. The difference increases with decreasing beam energy. Baryons show a larger difference compared to mesons. The relative values of v_2 for charged pions have the opposite trend to the values of charged kaons. It is concluded that, at the lower energies, particles and antiparticles are no longer consistent with the single NCQ scaling that was observed for $\sqrt{s_{NN}} = 200$ GeV. However, for the group of particles the NCQ scaling holds within $\pm 10\%$ while for the group of antiparticles the difference between baryon and meson v_2 continues to decrease to

lower energies. We further observed that the ϕ meson v_2 at the highest measured $m_T - m_0$ value is low compared to other hadrons at $\sqrt{s_{NN}} = 7.7$ and 11.5 GeV with 1.8σ and 2.3σ, respectively.

[1] D. J. Gross, R. D. Pisarski, and L. G. Yaffe, Rev. Mod. Phys. **53**, 43 (1981).

[2] C. Aktas and I. Yilmaz, Gen. Relativ. Gravit. **43**, 1577 (2011).

[3] M. M. Aggarwal *et al.* (STAR Collaboration), arXiv:1007.2613.

[4] A. M. Poskanzer and S. A. Voloshin, Phys. Rev. C **58**, 1671 (1998).

[5] S. Voloshin and Y. Zhang, Z. Phys. C **70**, 665 (1996).

[6] J. Adams *et al.* (STAR Collaboration), Phys. Rev. Lett. **95**, 122301 (2005).

[7] B. I. Abelev *et al.* (STAR Collaboration), Phys. Rev. C **75**, 054906 (2007).

[8] S. A. Voloshin, A. M. Poskanzer, and R. Snellings, arXiv:0809.2949.

[9] A. Adare *et al.* (PHENIX Collaboration), Phys. Rev. C **85**, 064914 (2012).

[10] C. Adler *et al.* (STAR Collaboration), Phys. Rev. Lett. **87,** 182301 (2001).

[11] J. Adams *et al.* (STAR Collaboration), Phys. Rev. Lett. **92,** 052302 (2004).

[12] P. Huovinen, P. F. Kolb, U. W. Heinz, P. V. Ruuskanen, and S. A. Voloshin, Phys. Lett. B **503,** 58 (2001).

[13] C. Nonaka, R. J. Fries, and S. A. Bass, Phys. Lett. B **583,** 73 (2004).

[14] T. Hirano and Y. Nara, Phys. Rev. C **69,** 034908 (2004).

[15] C. Shen and U. Heinz, Phys. Rev. C **85,** 054902 (2012); **86,** 049903(E) (2012).

[16] B. Schenke, S. Jeon, and C. Gale, Phys. Rev. Lett. **106,** 042301 (2011).

[17] M. Csanad, T. Csorgo, and B. Lorstad, Nucl. Phys. **A742,** 80 (2004).

[18] D. Molnar and S. A. Voloshin, Phys. Rev. Lett. **91,** 092301 (2003).

[19] K. H. Ackermann *et al.*, Nucl. Instrum. Methods Phys. Res., Sect. A **499,** 624 (2003).

[20] L. Adamczyk *et al.* (STAR Collaboration), Phys. Rev. C **86,** 054908 (2012).

[21] L. Adamczyk *et al.* (STAR Collaboration), arXiv:1301.2348.

[22] H. Masui and A. Schmah, arXiv:1212.3650.

[23] F. Wang, M. Nahrgang, and M. Bleicher, Phys. Rev. C **85,** 031902 (2012).

[24] J. Beringer *et al.* (Particle Data Group Collaboration), Phys. Rev. D **86,** 010001 (2012).

[25] J. C. Dunlop, M. A. Lisa, and P. Sorensen, Phys. Rev. C **84,** 044914 (2011).

[26] J. Steinheimer, V. Koch, and M. Bleicher, Phys. Rev. C **86,** 044903 (2012).

[27] J. Xu, L.-W. Chen, C. M. Ko, and Z.-W. Lin, Phys. Rev. C **85,** 041901 (2012).

[28] T. Song, S. Plumari, V. Greco, C. M. Ko, and F. Li, arXiv:1211.5511.

[29] Y. Burnier, D. E. Kharzeev, J. Liao, and H.-U. Yee, Phys. Rev. Lett. **107,** 052303 (2011).

[30] X. Dong, S. Esumi, P. Sorensen, N. Xu, and Z. Xu, Phys. Lett. B **597,** 328 (2004).

[31] A. Sibirtsev, H.-W. Hammer, U.-G. Meissner, and A. W. Thomas, Eur. Phys. J. A **29,** 209 (2006).

[32] B. Mohanty and N. Xu, J. Phys. G **36,** 064022 (2009).

[33] M. Nasim, B. Mohanty, and N. Xu, arXiv:1301.1375.